Geometry and Power Optimization of Coilgun Based on Adaptive Genetic Algorithms

Xi Tao, Shuhong Wang, *Senior Member, IEEE*, Youpeng Huangfu, Song Wang, and Yuqiong Wang

***Abstract*— A coilgun is an electromagnetic launcher based on electromagnetic induction. The projectile with a heavy load can be accelerated to a high speed. The currents that flow through the driving coils and the projectile would produce joule losses. All of the properties are drastically determined by the geometry and power of a coilgun. This paper aims to optimize the geometry and power parameters of the coilgun. The muzzle velocity is selected to be the objective when the temperature rise limitations are taken into consideration. To analyze the performance, an equivalent circuit model including the calculation of temperature rises is employed. The performance of a three-stage coilgun is calculated based on this model and then this coilgun is optimized with the utility of adaptive genetic algorithm taking the influence of temperature rise into consideration. The result of optimization shows that the muzzle velocity is improved and the temperature rises are conformed to the design requirements. The optimized coilgun is simulated by the finite-element method to verify the performance.**

***Index Terms*— Adaptive genetic algorithms (AGAs), coilgun, muzzle velocity, optimization, temperature rise.**

I. Introduction

ASYNCHRONOUS induction coilgun is a new kind of launch technology. The coilgun is made up of a projectile, driving coils, and sources. The materials of the projectile and driving coils are metals. A glass tube separates the projectile from the driving coils. Therefore, there is no contact between the projectile and the driving coils. The coilgun has a wide application prospect [1] due to the advantage that the projectile with a heavy load can be accelerated to a high speed by the electromagnetic force.

The USA is at a leading position in the field of electromagnetic launch. As early as the 1990s, Sandia National Laboratories conducted a series of experiments. A six-stage coilgun with 5-kg projectile is accelerated to a velocity of 335 m/s [2]. A 340-g projectile is accelerated to 406 m/s [3]. An electromagnetic launcher accelerates a 650 kg sled to 12 m/s [4]. In China, tests are also conducted. A 15-stage coilgun is designed to accelerate a 5-kg projectile to 220 m/s [5].

Manuscript received October 15, 2014; revised February 11, 2015; accepted February 17, 2015.

X. Tao, S. Wang, Y. Huangfu, and S. Wang are with the State Key Laboratory of Electrical Insulation and Power Equipment, School of Electrical Engineering, Xi'an Jiaotong University, Xi'an 710049, China (e-mail: taoxi_xjtu@163.com; shwang@mail.xjtu.edu.cn; 708810661@qq.com; 312616561@qq.com).

Y. Wang is with the Golisano College of Computing and Information Sciences, Rochester Institute of Technology, Rochester, NY 14623 USA (e-mail: 416714538@qq.com).

Color versions of one or more of the figures in this paper are available online at http://ieeexplore.ieee.org.

Digital Object Identifier 10.1109/TPS.2015.2406778

The launch is a complex process, which contains the kinetic analysis, electromagnetic analysis, and thermal analysis. To analyze the performance, two numerical models, the circuit model and the field model are applied. The current filament method is widely used due to its simple principle and easy realization [6]. An improved current filament method is established to achieve more accurate performance [7]. Software packages such as WARP-10 [8], AXICOIL [9], and SLINGSHOT [3], [10] are developed. To develop the performance of the coilgun, optimizations are conducted based on the current filament method [11], [12].

This paper focuses on the muzzle velocity and the temperature rises of coilgun. The equivalent circuit model including the calculation of temperature rises is used to gain the performance of coilgun. A three-stage coilgun is calculated with the equivalent circuit model. To improve the performance of this coilgun, an adaptive genetic algorithm (AGA) is used to optimize the geometry and power of the coilgun. The temperature rises of the projectile and driving coils would weaken the mechanical strength of materials and even melt the materials. In this case, the temperature rises are important parameters, which should be limited. The result of optimization indicates that the muzzle velocity and the temperature rise increase compared with those before optimization. To verify the result, this three-stage coilgun and optimization are simulated by the finite-element method (FEM). The simulations show that the calculations by the current filament method are credible.

II. Current Filament Method

A coilgun mainly consists of the driving coils and the projectile, which can be considered as coaxial coils. The eddy currents flowing through the projectile are induced due to the eddy effect. The interactions of the currents flowing through both the projectile and the driving coils lead to the electromagnetic force. The projectile is split into subcoils based on the current filament method. To achieve the accurate performance, the closer to the driving coils, the smaller the area of the subcoil is. Each subcoil is a hoop with the rectangular cross section. The current flowing through the same hoop is regarded to be uniform. Each hoop is an independent element.

To analyze the performance of coilgun conveniently, an axisymmetric model is set up. Fig. 1 shows the model in the cylindrical coordinate and z-direction is the direction of the axis. According to the model, an equivalent circuit that contains a hoop and a driving coil is built up. Fig. 2 shows the equivalent circuit. The capacitor bank provides energy for the driving coil.

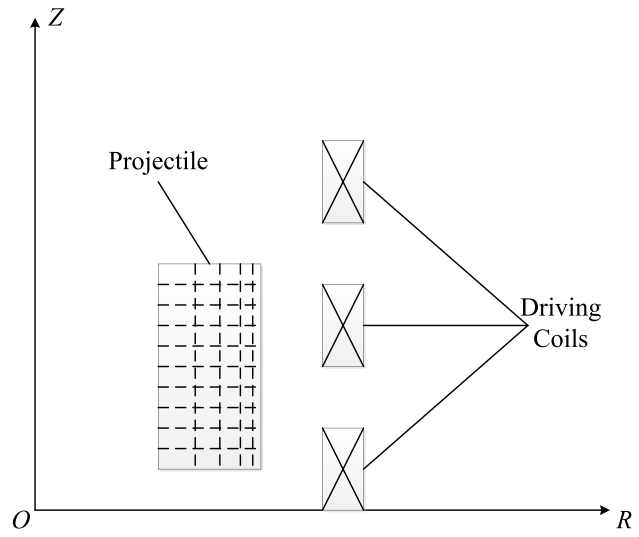

Fig. 1. Axisymmetric model of coilgun in the cylindrical coordinate.

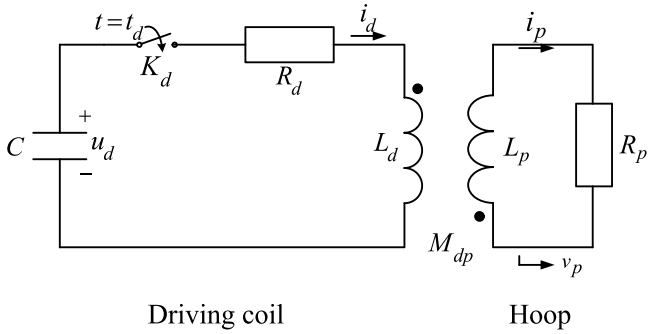

Fig. 2. Equivalent circuit model of a hoop and a driving coil.

According to Kirchhoff's voltage law, the equivalent circuit in Fig. 2 can be described as

$$u_d = i_d R_d + L_d \frac{di_d}{dt} + M_{\mathrm{dp}} \frac{di_p}{dt} + i_p \frac{dM_{\mathrm{dp}}}{dz} v \tag{1}$$

$$0 = i_p R_p + L_p \frac{di_p}{dt} + M_{\mathrm{dp}} \frac{di_d}{dt} + i_d \frac{dM_{\mathrm{dp}}}{dz} v \tag{2}$$

where u_d is the voltage of capacitor bank, R_d is the resistance of the driving coil, L_d is the self-inductance of the driving coil, i_d is the current of the driving coil, R_p is the resistance of the hoop, L_p is the self-inductance of the hoop, i_p is the current of the hoop, M_{dp} is the mutual inductance between the driving coil and the hoop, and v is the velocity of the projectile.

When we take all the driving coils and the hoops into consideration in the equivalent circuit model, (1) and (2) can be rewritten as

$$\{[L] + [M]\} \frac{d[I]}{dt} = [V_c] - [R][I] - v\left[\frac{d[M]}{dz}\right] \cdot [I] \tag{3}$$

where $[L]$ is the self-inductance matrix, $[M]$ is the mutual inductance matrix, $[I]$ is the current column matrix, $[V_c]$ is the voltage column matrix of the capacitor banks, $[R]$ is the resistance matrix, and v is the velocity of the projectile.

The currents that flow through the capacitor banks are also the currents of the driving coils. The relationship between currents and voltages in the capacitor banks is

$$[C] \frac{d[V_c]}{dt} = -[I_d] \tag{4}$$

where $[C]$ is the capacitance column matrix and $[I_d]$ is the current column matrix of the driving coil.

The electromagnetic force can be calculated based on the currents of driving coils and hoops. According to Newton's second law of motion, the equation is

$$M_p \frac{dv}{dt} = \sum_{p=1}^{m} \sum_{d=1}^{n} I_p I_d \frac{dM_{pd}}{dz} \tag{5}$$

where M_p is the mass of the projectile and z is the position of the projectile.

The relationship between the velocity and position of the projectile is given by

$$\frac{dz}{dt} = v. \tag{6}$$

The current densities of driving coils and hoops are

$$[J] = \frac{[I]}{S} \tag{7}$$

where S is the section area and $[J]$ is the column matrix of current density.

The period of launching process is short. The boundaries among the hoops are considered to be adiabatic. According to Joule's law, the heating power is

$$[W] = \frac{[J^2]}{\gamma} \tag{8}$$

where γ is the resistivity and $[W]$ is the column matrix of heating power.

III. Three-Stage Coilgun

A three-stage coilgun is designed. The projectile is made of aluminum and the driving coils are made of copper. The length of the projectile is 203 mm. The thickness of the projectile is 15 mm. The outer radius of the projectile is 70 mm. The inner radius of the driving coil is 73.5 mm. There are two layers of wires in each driving coil and there are 19 turns in each layer. The capacitances of capacitor banks are 0.020485, 0.005863, and 0.002059 F, respectively. The initial voltages of capacitor banks are 4600, 9100, and 14 700 V, respectively. Fig. 3 shows the geometry of this coilgun. The initial velocity of the projectile is 11.9 m/s. The distance between the adjacent driving coils is 28 mm. The cross-sectional area of the wire used in the driving coils is 4 mm × 4 mm. The insulation thickness of the wire used in the driving coils is 0.82 mm. Thus, the cross-sectional area with the insulation of the wire in the driving coils is 5.64 mm × 5.64 mm.

This three-stage coilgun is calculated using the equivalent circuit model. The muzzle speeds of three stages are 81.97, 144.32, and 226.25 m/s, respectively. Fig. 4 shows the speed of the projectile.

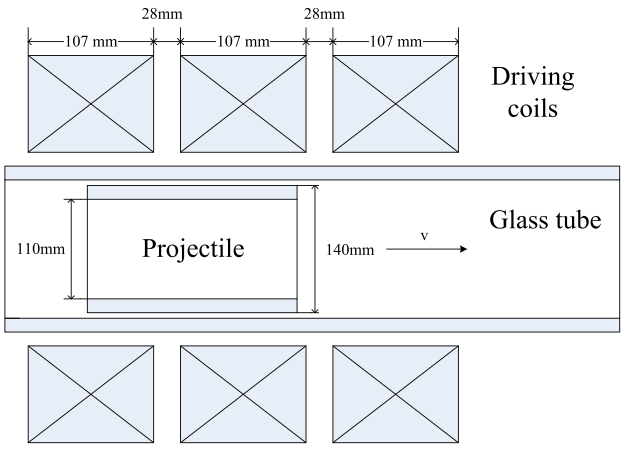

Fig. 3. Geometry of a three-stage coilgun.

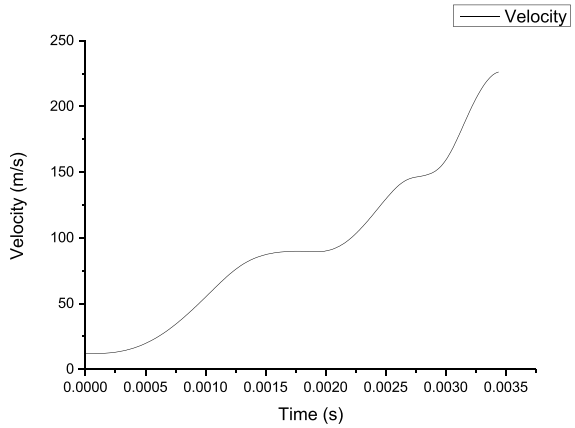

Fig. 4. Speed of the projectile.

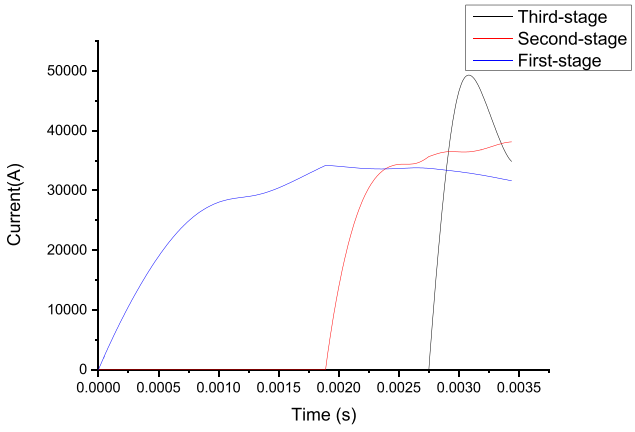

Fig. 5. Currents of driving coils.

The currents flowing through the driving coils are shown in Fig. 5. The peak currents of three stages are 34.20, 38.14, and 49.32 kA, respectively.

The temperature rises are calculated based on (7) and (8). The temperature rises of the three driving coils are 55.86, 31.68, and 20.63 K, respectively. The maximum temperature rise in the coils is 255.71 K. Fig. 6 shows the current of the hoop, whose temperature rise approaches the maximum value.

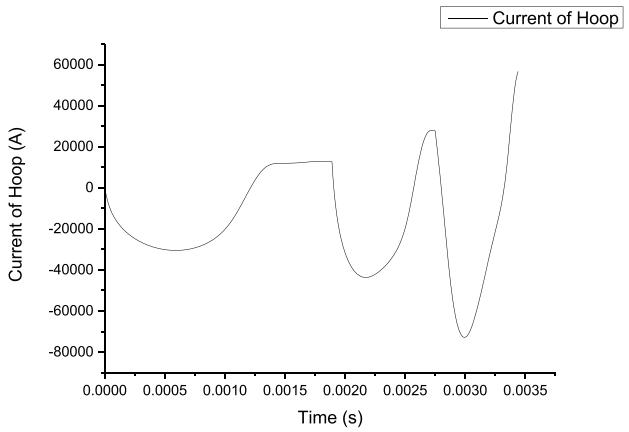

Fig. 6. Current of the hoop whose temperature rise is maximum.

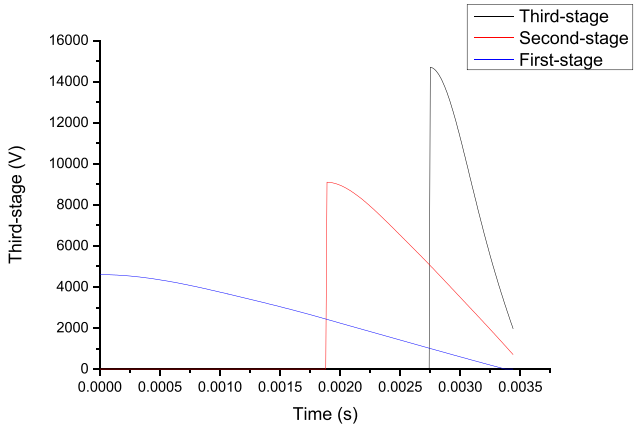

Fig. 7. Voltages of capacitor banks.

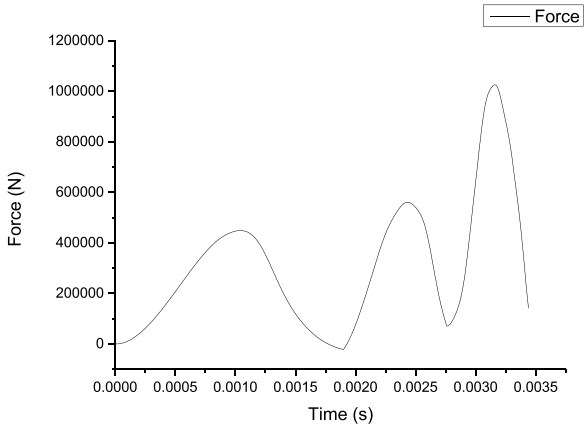

Fig. 8. Electromagnetic force of the projectile.

The voltages of capacitor banks are shown in Fig. 7. Fig. 8 shows the electromagnetic force of the projectile.

IV. Adaptive Genetic Algorithm

Genetic algorithm (GA) is a programming technique, which mimics biological evolution as a problem-solving strategy and GA is an effective optimization method. To improve this method, many variants of canonical GAs are proposed. AGA is one of these methods.

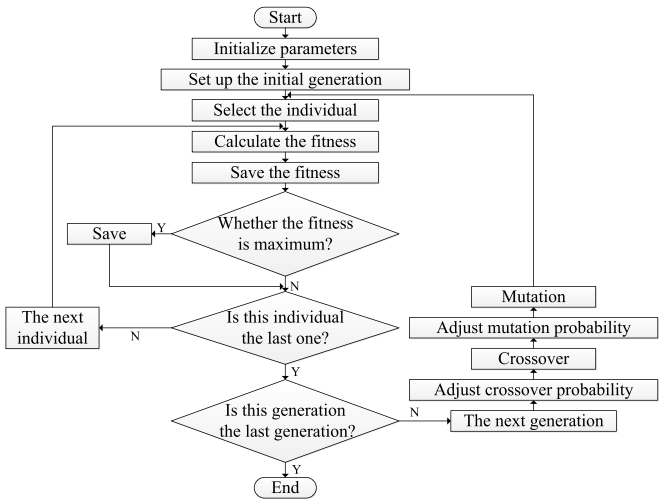

Fig. 9. Flowchart of AGA.

Crossover and mutation probabilities are very important parameters of GA and even directly affect the convergence of the algorithm. Crossover is a process of taking more than one parent solution and producing a child solution from them. Mutation alters one or more gene values in the chromosome from its initial state. Mutation probability should be set low. If the mutation probability is set too high, the search will turn into a primitive random search. To find better crossover and mutation probabilities, AGA makes crossover and mutation probabilities depending on the fitness.

The process of AGA contains coding, fitness calculation, selection, reproduction, crossover, mutation, and decoding. The flowchart of AGA is shown in Fig. 9. The method sets potential solution to a specific problem, and a fitness function allows each candidate to be evaluated. The outstanding individuals would be retained to the next generation. Then, the crossover and mutation probabilities are calculated in each generation based on the fitness.

A. Population Size and Generation

In the optimization of this three-stage coilgun, the population size is set as 100 to balance the optimization effect and the performance of computer. In addition, the generation is set as 15 to achieve a stable solution.

B. Design Parameters

In the optimization of this three-stage coilgun, the selected design parameters would be divided into three groups. The first group contains the length, the thickness, and the outer diameter of the projectile. The second group consists of the number of turns, the spacing, and the trigger position of the driving coils. Finally, the third group comprises the initial voltages and capacitances of capacitor banks. Table I shows the ranges of selected design parameters.

TABLE I
RANGES OF DESIGN PARAMETERS

Component	Parameter	Value range
Projectile	Length	50-300/mm
	Thickness	5-30/mm
	Outer diameter	70-100/mm
Driving coils	Number of turns	10-30
	Spacing	10-100/mm
	Trigger position	/
Capacitor banks	Initial voltage	5000-10000/V
		10000-15000/V
		15000-20000/V
	Capacitance	0.01-0.02/F
		0.005-0.01/F
		0.001-0.005/F

The range of trigger position is determined after the geometry of coilgun is established.

C. Fitness Function

The objective of optimization is to achieve a better acceleration performance, so the muzzle velocity is selected as the fitness function

$$\max f = v \tag{9}$$

where f is the fitness and v is the muzzle velocity.

D. Constraints

In the optimization, the temperature rises of the driving coils and hoops should be limited to the melting points of materials. The melting points of copper and aluminum are 1084 °C and 660 °C, respectively

$$\text{s.t.} \begin{cases} T_c < 1084 \text{ K} \\ T_h < 660 \text{ K} \end{cases} \tag{10}$$

where T_c is the maximum temperature rise of the driving coil and T_h is the maximum temperature rise of the hoop.

E. Selection

Roulette wheel selection is a common method in GA. In this method, the probability is proportional to the fitness

$$p_i = \frac{f_i}{\sum_{i=1}^{N} f_i}, \quad i = 1, 2, \ldots, N \tag{11}$$

where p_i is the probability of selection for the individuals.

F. Crossover

To achieve a better optimizing performance than the traditional GA, the crossover probability in each generation is variable. If the fitness is less than the average fitness, a higher crossover probability is set. On the contrary, a higher fitness leads to a small crossover probability. The crossover probability is

$$p_c = \begin{cases} 0.9 - \dfrac{0.3 \times (f - f_{\text{avg}})}{f_{\max} - f_{\text{avg}}} & f \geq f_{\text{avg}} \\ 0.9 & f < f_{\text{avg}} \end{cases} \tag{12}$$

where p_c is the crossover probability, f is the fitness of current individual, f_{avg} is the average fitness in this generation, and $f_{\max}$ is the maximum fitness value in this generation.

TABLE II
OPTIMAL RESULTS

Component	Parameter	Value
Projectile	Length	228.50mm
	Thickness	16.75mm
	Outer diameter	87.28mm
Driving coils	Number of turns	13
		27
		20
	Spacing	0mm
		77.41mm
		82.54mm
	Trigger position	36.66mm
		91.75mm
		321.21mm
Capacitor banks	Initial voltage	6215V
		14475V
		18870V
	Capacitance	0.01901F
		0.00657F
		0.00396F

G. Mutation

The selection of mutation probability is the same as the selection of crossover probability. A small fitness leads to a higher mutation probability. If the fitness is less than the average fitness, the mutation probability is as much as 10%. The mutation probability is

$$p_m = \begin{cases} 0.1 - \dfrac{0.099 \times (f_{\max} - f)}{f_{\max} - f_{\text{avg}}} & f \geq f_{\text{avg}} \\ 0.1 & f < f_{\text{avg}} \end{cases} \tag{13}$$

where p_m is the mutation probability.

V. OPTIMAL RESULTS

An optimized coilgun is obtained with AGA. Table II shows the results of design parameters, including the parameters of projectile, driving coils, and capacitor banks.

The muzzle speeds of the projectile in each stage of the optimization are 100.59, 309.41, and 399.46 m/s, which are greatly improved than those before optimization. Fig. 10 shows the speeds before and after optimization. The initial voltages of capacitor banks increased about 20%–25%. The final muzzle velocity of the three-stage coilgun increased almost 77%.

The electromagnetic forces before and after optimization are shown in Fig. 11. It is obvious that optimized coilgun has a better performance in acceleration.

The currents of the driving coils are shown in Fig. 12. The maximum currents of three driving coils are 52.98, 54.97, and 54.57 kA, respectively. The maximum temperature rises in each stage are 98.73, 45.74, and 16.87 K. The maximum temperature rise of the first driving coil is increased from 55.86 to 98.73 K. The maximum temperature rise of the hoop is rapidly increased from 255.71 to 422.81 K. Fig. 13 shows the currents of the hoop with the maximum temperature rise.

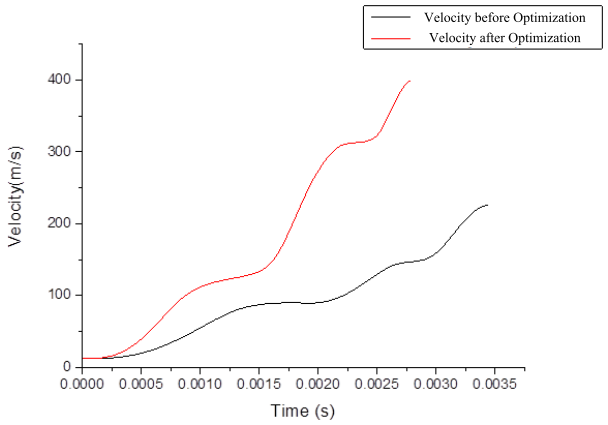

Fig. 10. Speeds of the projectile.

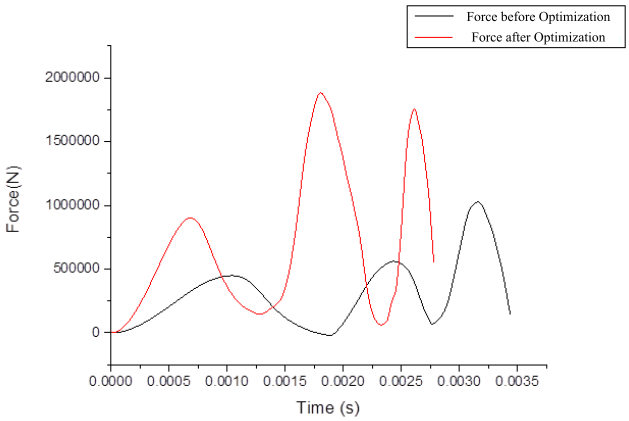

Fig. 11. Electromagnetic forces of the projectile.

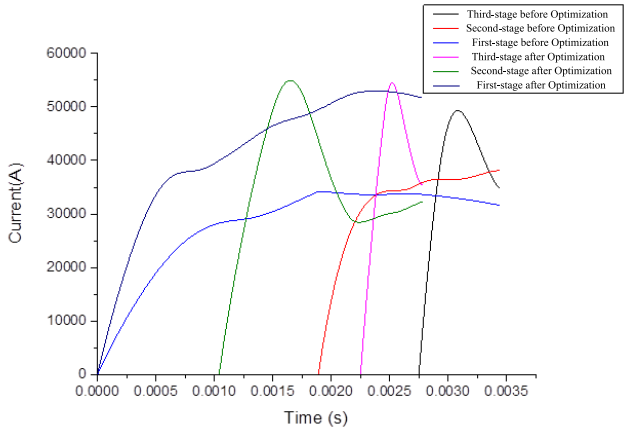

Fig. 12. Currents of driving coils.

VI. SIMULATION

To verify the optimization results, a simulation is conducted in ANSYS MAXWELL 15.0 [13], a commercial finite element package. Fig. 14 shows the finite element geometric model that has the projectile, the driving coils, moving band, and solving area. The switch is turn-ON by the position of the projectile to control the discharges of capacitor banks.

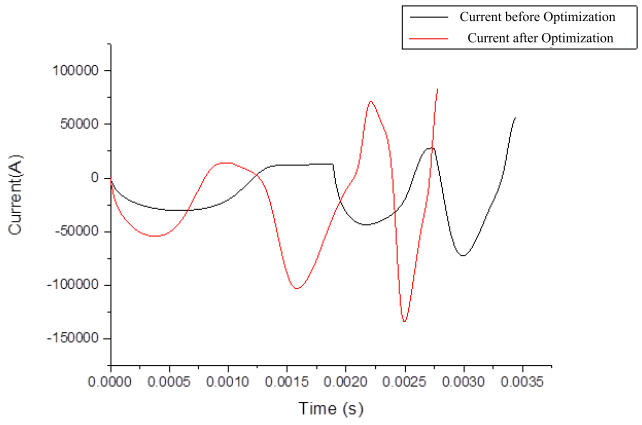

Fig. 13. Currents of the hoop with the maximum temperature rise.

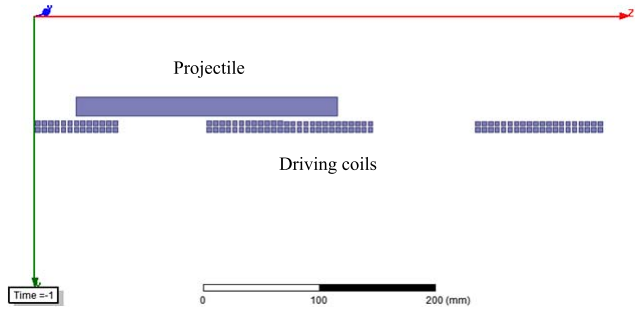

Fig. 14. Geometric model in ANSYS MAXWELL 15.0.

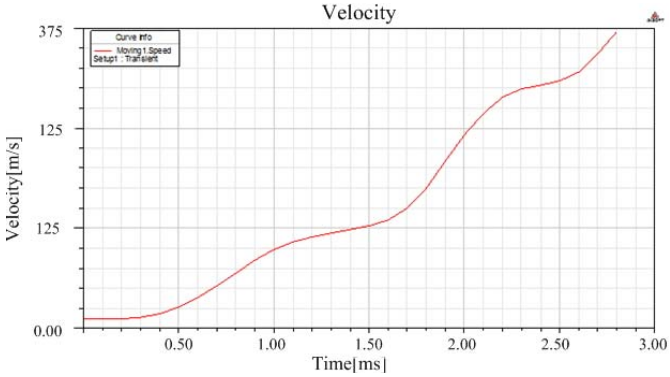

Fig. 15. Speed curve of the projectile in simulation.

After the simulation, Fig. 15 presents the speed of the projectile. The muzzle velocity is 374.70 m/s. The launching process is shorter than 3 ms. In such a short time, the projectile is accelerated to a very high speed due to the electromagnetic force. Fig. 16 shows the electromagnetic force.

The currents of the driving coils are calculated in the simulation. Fig. 17 presents the currents of the driving coils. The maximum currents are 51.35, 53.57, and 46.83 kA. Fig. 18 shows the joule losses at the end time of launch. The maximum temperature rise is at the bottom of the projectile near the driving coil. This result is consistent with the result calculated by the equivalent circuit model. The results of this simulation verify the correctness of the optimization results.

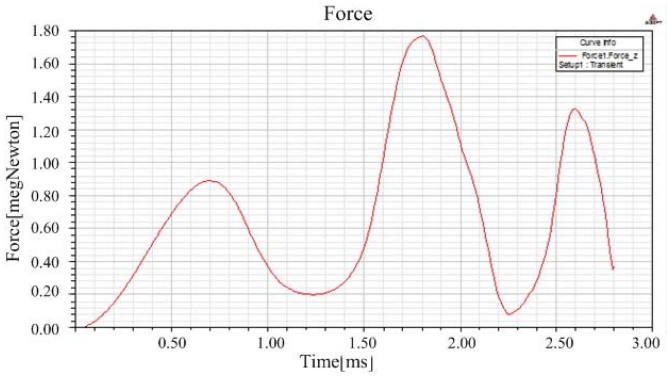

Fig. 16. Force curve of the projectile in simulation.

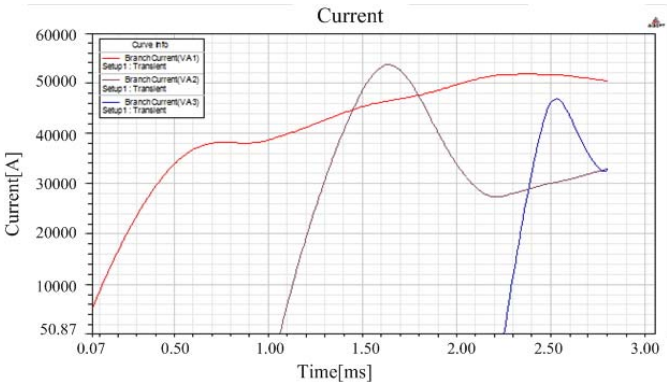

Fig. 17. Current curves of driving coils in simulation.

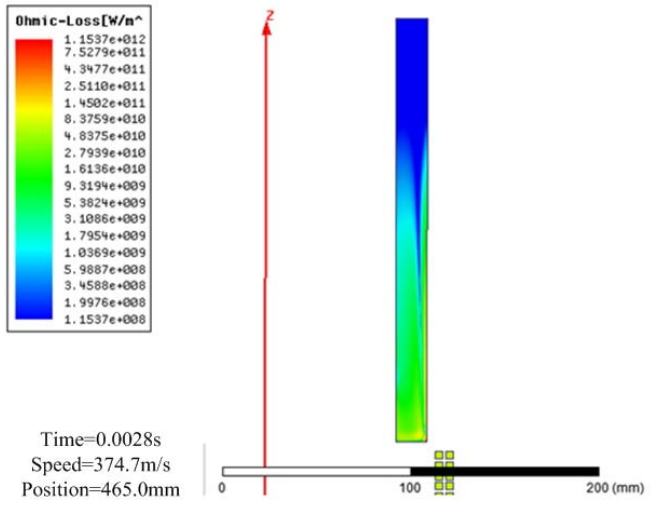

Fig. 18. Joule losses of the projectile in simulation.

The error of the muzzle velocity is about 6.2%. In this case, the optimization results are credible compared with the results of the simulation.

VII. Conclusion

Coilgun is an effective launch device based on the electromagnetic energy. In this paper, the current filament method greatly simplifies the calculation of coilgun. AGA is applied to optimize a three-stage coilgun. The geometry and

power of this coilgun are selected to be the design parameters. The temperature rises are considered as the constraints. After the optimization, though the maximum temperature rise of the projectile increases 65.35% from 255.71 to 422.81 K, the muzzle velocity of the projectile is improved 76.56%. The temperature rapidly increases in a short time and has a great influence on the process of launching.

The results of the optimization suggest that the muzzle velocity can be improved and the temperature rises are satisfied with the constraints. To validate the results of the optimization, a simulation is conducted using FEM. The results of the simulation indicate the optimization is credible and accurate.

REFERENCES

[1] W. Ying, R. A. Marshall, and C. Shukang, *Physics of Electric Launch*. Beijing, China: Science Press, 2004, pp. 136–150.

[2] R. J. Kaye, E. L. Brawley, B. W. Duggin, E. C. Cnare, D. C. Rovang, and M. M. Widner, "Design and performance of a multi-stage cylindrical reconnection launcher," *IEEE Trans. Magn.*, vol. 27, no. 1, pp. 596–600, Jan. 1991.

[3] R. J. Kaye *et al.*, "Design and performance of Sandia's contactless coilgun for 50 mm projectiles," *IEEE Trans. Magn.*, vol. 29, no. 1, pp. 680–685, Jan. 1993.

[4] M. S. Aubuchon, T. R. Lockner, and B. N. Turman, "Results from Sandia National Laboratories/Lockheed Martin electromagnetic missile launcher (EMML)," in *Proc. 15th IEEE Int. Pulsed Power Conf.*, Jun. 2005, pp. 75–78.

[5] T. Zhang, W. Guo, H. Zhang, B. Cao, K. Huang, and R. Ren, "Design and testing of a 15-stage synchronous induction coilgun," in *Proc. 16th Int. Symp. Electromagn. Launch Technol. (EML)*, May 2012, pp. 1–4.

[6] J. He, E. Levi, Z. Zabar, and L. Birenbaum, "Concerning the design of capacitively driven induction coil guns," *IEEE Trans. Plasma Sci.*, vol. 17, no. 3, pp. 429–438, Jun. 1989.

[7] L. Shoubao, R. Jiangjun, P. Ying, Z. Yujiao, and Z. Yadong, "Improvement of current filament method and its application in performance analysis of induction coil gun," *IEEE Trans. Plasma Sci.*, vol. 39, no. 1, pp. 382–389, Jan. 2011.

[8] M. M. Widner, "WARP-10: A numerical simulation model for the cylindrical reconnection launcher," *IEEE Trans. Magn.*, vol. 27, no. 1, pp. 634–638, Jan. 1991.

[9] J. A. Andrews and J. R. Devine, "Armature design for coaxial induction launchers," *IEEE Trans. Magn.*, vol. 27, no. 1, pp. 639–643, Jan. 1991.

[10] I. R. Shokair, M. Cowan, R. J. Kaye, and B. M. Marder, "Performance of an induction coil launcher," *IEEE Trans. Magn.*, vol. 31, no. 1, pp. 510–515, Jan. 1995.

[11] L. Guo *et al.*, "Optimization for capacitor-driven coilgun based on equivalent circuit model and genetic algorithm," in *Proc. IEEE Energy Convers. Congr. Expo. (ECCE)*, Sep. 2009, pp. 234–239.

[12] Y. Zhang, K. Liu, J. Liao, Y. Zhang, C. Wu, and Y. Hu, "Parameter optimization of multi-stage coilgun using orthogonal test approach," in *Proc. 16th Int. Symp. Electromagn. Launch Technol. (EML)*, May 2012, pp. 1–6.

[13] ANSYS. *ANSYS MAXWELL 15.0 Software Package*. [Online]. Available: http://www.ansys.com/, accessed Aug. 8, 2014.

Xi Tao was born in Xi'an, China, in 1991. He received the B.S. degree in electrical engineering from Xi'an Jiaotong University, Xi'an, in 2013, where he is currently pursuing the M.S. degree in electrical engineering.

His current research interests include optimization algorithms and harmonic suppression.

Shuhong Wang (SM'13) was born in Xi'an, China, in 1968. He received the B.S. degree, the M.S. degree, and the Ph.D. degree in electrical engineering from Xi'an Jiaotong University, Xi'an, in 1990, 1993, and 2002, respectively.

He was a Post-Doctoral Fellow with the Department of Mechatronics, Gwangju Institute of Science and Technology, Gwangju, Korea, from 2004 to 2005, a Research Fellow with the Faculty of Engineering, University of Technology at Sydney, Sydney, NSW, Australia, in 2005, and a Visiting Professor with the Faculty of Engineering and Information Technology, University of Technology at Sydney, from 2008 to 2009. His current research interests include the theory of circuit, electromagnetic field, and multiphysics field, numerical analysis methods, the design, simulation, and optimization of energy-efficient power conversion and transmission equipment and special electromagnetic devices, modeling and simulation of the electromagnetic properties of advanced electrical materials, including superconducting materials, and magnetic materials, and the applied technology of superconducting power applications.

Youpeng Huangfu was born in Shangqiu, China, in 1987. He received the B.S. degree in electrical engineering and automation from Jilin University, Changchun, China, in 2012. He is currently pursuing the Ph.D. degree in electrical engineering from Xi'an Jiaotong University, Xi'an, China.

His current research interests include high-altitude nuclear electromagnetic pulse, lightning electromagnetic pulse, electromagnetic compatibility, and simulation method of narrow electromagnetic impulse in time domain.

Song Wang was born in Weinan, Shannxi, China, in 1989. He received the B.S. degree in electrical engineering from the Dalian University of Technology, Dalian, China, in 2012. He is currently pursuing the M.S. degree in electrical engineering with Xi'an Jiaotong University, Xi'an, China.

His current research interests include biological electromagnetism.

Yuqiong Wang received the B.S. degree from Wuhan University, Wuhan, China, in 2005. She is currently pursuing the M.S. and Ph.D. degrees with the Rochester Institute of Technology, Rochester, NY, USA.